

MODELLING LONG-TERM SOLAR IRRADIANCE VARIABILITY: A NEW APPROACH; PART 1: STUDY THE ERROR DISTRIBUTION IN SOLAR IRRADIANCE AND GROUND-BASED SURROGATES

J.M. Pap, A. Vigouroux and Ph. Delache

J.M. Pap: Jet Propulsion Laboratory, California Institute of Technology, MS 169-506, 4800 Oak Grove Dr., Pasadena, CA 91109, U.S.A.

A. Vigouroux, and Ph. Delache¹: Laboratoire Cassini, associé au C. N.R.S. (U.R.A. 1362), Observatoire de la Côte d'Azur, 1117-229, F-06304, NICE Cédex 04, FRANCE

Abstract

Analyses based on 11 irradiance observations from space within the last one and a half decades have discovered variations in the entire solar spectrum and at UV wavelengths on time scales of minutes to decades. Although considerable information has been gathered on the observed irradiance changes, it has become clear that there is a residual irradiance variability that is not explained by sunspots, photospheric faculae and chromospheric plages, and the magnetic network. Because of the lack of quantitative physical models of the solar radiative output, the current irradiance "models" have been developed with a simple linear regression analysis which is not capable of distinguishing between periodic or seasonal irradiance components and their error-terms. This paper estimates the degree of significance of the observed variations in solar total and UV irradiances and their magnetic surrogates and to provide irradiance estimates based on the significant solar components. In this part of the paper (Paper 1) the results of error distributions (both instrumental and solar noise) in solar irradiance and its ground-based surrogates are presented.

¹Died 011 October 13, 1994

1. Introduction

For more than one and a half decades, solar irradiance (both bolometric and at different wave lengths) has been observed from different satellites. These irradiance observations led to the discovery of changes in solar total and UV irradiances on ‘till)’ scales from minutes to decades (e.g. Hudson, 1988; Lean, 1991). It has been shown that the solar energy flux varies in parallel with the solar magnetic activity cycle, being higher during maximum solar activity conditions. The long-term irradiance variations over the solar cycle are attributed to the changing emission of bright faculae and the magnetic network (e.g. Lean, 1987). The short-term variations (on the solar rotational time scale) in UV irradiance are related to the bright plages as they evolve and move across the solar disk (Lean, 1987) and to a lesser extent to the bright magnetic network (Pap et al., 1990). The short-term variability observed in the entire solar flux is more complex and it is primarily determined by the combined effect of dark sunspots and bright faculae (Willson et al., 1981).

Although considerable information exists on solar irradiance variability, it has become clear that not all the observed irradiance changes can be explained by sunspots, faculae/plages, and the magnetic network (e.g. Pap and White, 1994). While there is a reasonably good agreement between measured total solar and UV irradiances and their model estimates calculated from observations of dark sunspots bright magnetic features during the declining portion of solar cycle 21 and the rise of solar cycle 22, there is a breakdown between the observed and modelled irradiance values during maximum and minimum solar activity conditions. It has been shown that the modelled total irradiance values underestimate the observed changes at the maximum of solar cycle 21 (Joukalanen and Lean, 1988; Willson and Hudson, 1991) and solar cycle 22 (Pap et al., 1994; Brandt et al., 1994). In the case of UV irradiance, the irradiance models cannot account for the slow decrease in UV irradiance during solar minimum activity conditions. While most of the solar indices show a flat solar minimum background variability between 1984 and 1987, the UV irradiance slowly decreased towards 1986 and started to rise with the growing activity of solar cycle 22 in early 1987 (Donnelly, 1989; Barth et al., 1989; Pap et al., 1991). Furthermore, the “remaining part” of the irradiance power spectra after removing the effect of sunspots and bright magnetic features, including faculae, plages and the magnetic network, has peaks around 9, 13.5, 27 and 300 days (Fröhlich and Pap, 1989; Pap and Fröhlich, 1992; Pap, 1992), and the amplitude of this residual variability depends on the phase of the solar cycle (Pap and Fröhlich, 1992). It has not been clarified yet whether these discrepancies between the observed and calculated irradiance data are simply related to measuring uncertainties (in both irradiance and ground-based surrogates) or they characterize a real solar variability that may be related to global effects, such as large scale motions (Ribes et al., 1985) or photospheric temperature changes (Kuhn et al., 1988). Considering that the radiative output of the Sun is the main driver of the physical processes in the Earth’s atmosphere and its climate system, this problem has become one of the most important issues in solar-terrestrial physics. Besides

the climate implications of solar variability, the analysis of time correlation between solar irradiance and various solar parameters offers an additional 100] for studying the underlying physical processes inside the Sun.

Because of the lack of quantitative physical models of solar irradiance, the current models, developed with linear regression analyses, provide only a general information on the observed irradiance variations. It has been shown that the time series of solar irradiances, either space-borne or ground-based surrogates, can be regarded as “pseudo-periodic” signals with variable spectral properties (e.g. change of periods, amplitudes, and phases) (Lean and Repoff, 1987; Fröhlich and Pap, 1989; Pap et al., 1990a; Bower, 1992). The currently used empirical models developed with linear regression analyses cannot distinguish between periodic or seasonal irradiance components and an error-term describing the essentially random fluctuations of the time series about the trend and seasonal components (Priestly, 1993). Instead of a standard regression model, special techniques are required to determine the spectral properties of the investigated time series. However, the most commonly used spectral analysis (the Fourier analysis of the whole data set) can provide misleading information since the Fourier transform converts the whole signal to the frequency domain without, saving the local behavior of the time series. A relatively new technique: called wavelet analysis has been developed to study quasi-periodic or time-varying time series as a linear superposition of elementary basis functions -the wavelets- that are localized in time and frequency (Scargle, 1993). This technique has already been applied to study changes in the solar radius (Vigouroux and Delache, 1993) and the relative sunspot number (Vigouroux and Delache, 1994).

The basic question to be addressed in this paper is the degree of significance of the observed variations in solar total and UV irradiances as well as in their surrogates measuring solar magnetic activity. In order to interpret the results gained from various types of statistical analyses, it is essential to understand and evaluate the uncertainties in the data. Identification of random errors in the data sets provide an important clue to estimate the signal-to-noise ratio and to clarify whether the observed small residual variability in solar irradiance is simply determined by a noise component in the data or whether it clearly represents a real solar variability. On the other hand, in studying long-term irradiance variabilities, the short-term solar changes (less than the solar rotation period) can also be regarded as “noise” in the spectral analysis. The corresponding results on the error distribution (both instrumental and solar noise) of solar irradiance and its ground-based surrogates are described in this paper (thereafter Paper I), following the basic idea of Vigouroux and Delache (1994). In the second part (Paper II) the results of a time and frequency analysis with the wavelet technique will be presented. Since the wavelet transform is capable of taking care of unequal error bars determined from statistical properties of the data, the inverted wavelet transforms will provide better irradiance estimates based on the significant solar components.

2 Description of the data

Total solar irradiance, the integrated solar flux over the entire solar spectrum, has been measured from Earth space for over a decade. The direct space observations of total solar irradiance began in late November of 1978 by the Earth Radiation Budget (ERB) experiment on board the Nimbus-7 satellite that was terminated in January of 1993 (Kyle et al., 1993). The ERB experiment was a multipurpose experiment that included an electrically self-calibrating active cavity radiometer with an estimated at-launch accuracy of $\pm 0.5\%$ (Hickey et al., 1988). Limitations imposed on the ERB solar observations by the absence of solar pointing on the Nimbus platform sustained a noise level in the ERB results which was estimated as $\pm 0.03\%$ (Hoyt et al., 1992) and this low precision inhibited the recognition of intrinsic solar variability until subsequent detection by the Active Cavity Radiometer Irradiance Monitoring (ACRIM) experiment on board the SMM satellite (Willson et al., 1981). The high precision irradiance observations of the SMM/ACRIM radiometer started in February 1980. During the first 10 months of the ACRIM observations the measuring precision was so high ($\pm 0.002\%$) that each observed event had a solar, rather than an instrumental, origin (Willson, 1984). In December 1980 the solar-pointing system of the SMM satellite failed and it was placed into the so-called "spin-mode". During this operational mode until May 1984, when the SMM was repaired during a Space Shuttle Mission, the measuring precision decreased by about a factor of 5 (from 0.002% to 0.01%) (Willson, 1984). After May 1984 the original measuring precision was restored and the original high quality ACRIM total irradiance data were collected through November 1989 when the operation of the SMM satellite was terminated.

Extensive measurements of the solar ultraviolet irradiance have been made by the Solar Backscatter Ultraviolet (SBUV) experiment on the Nimbus-7 satellite between 160-400 nm from November 1978 through 1987 (Schlesinger and Cebula, 1992; Cebula et al., 1994) and by the NOAA9 and NOAA11/SBUV2 instruments since 1985 (Donnelly, 1991; Donnelly et al., 1994). The ratio in the core of the Mg 280 nm line to the irradiance at the neighboring continuum wavelengths (Mg II h & k core-to-wing ratio) has proved to be an accurate index of solar UV variability (Heath and Schlesinger, 1986). The Nimbus-7 and NOAA9 Mg core-to-wing ratios (Mg C/w) were made consistent by means of their overlapping observational time period in 1986, and also by means of the full disk Ca II H index (Donnelly, 1991). In order to directly compare the variations in total solar irradiance with the changes in the UV flux, the effect of sunspots have been removed from total irradiance by means of the Photometric Sunspot Index (Hudson et al., 1982; Fröhlich et al., 1994). The Photometric Sunspot Index (PSI) relates the observed sunspot areas and their contrast to a net effect on the radiative output of the observed solar hemisphere and it is corrected for the photospheric limb darkening. The original PSI function (Hudson et al., 1982) was calculated on the assumption that the area and temperature ratio of the umbra and penumbra are constant and therefore the PSI function was calculated on the basis of a constant contrast value of sunspots (details on the calculation of PSI

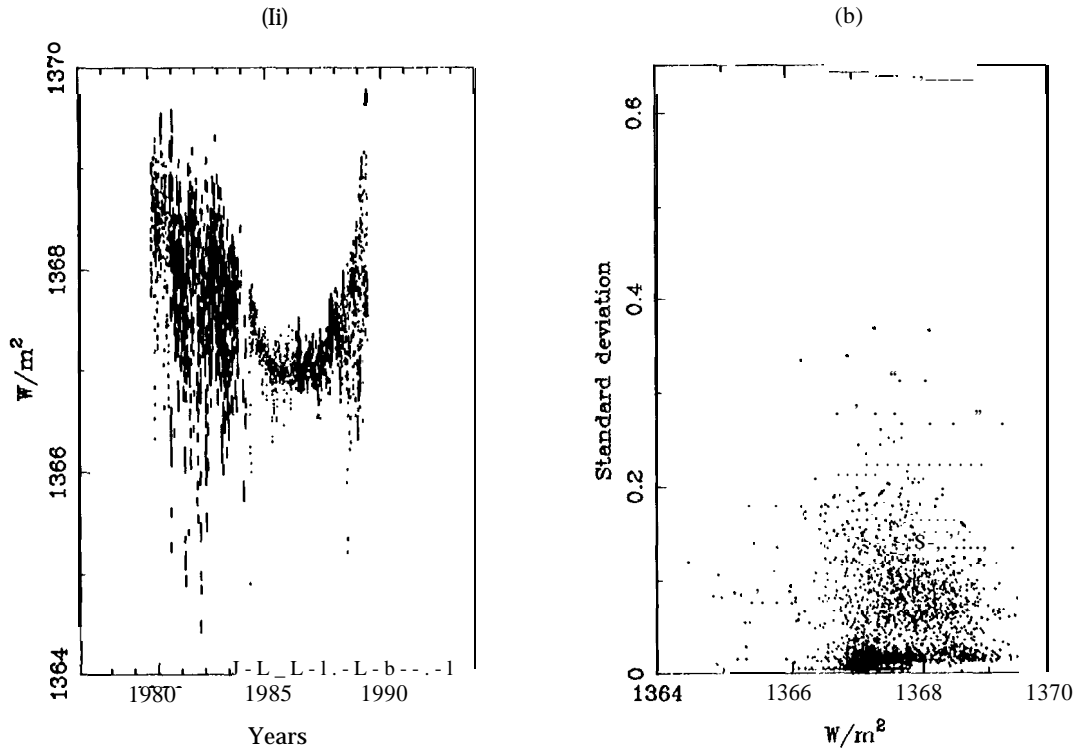


Figure 1: The daily mean values of the SMM/ACRIM 1 total solar irradiance are plotted together with their standard deviations (a). The standard deviations versus the daily ACRIM 1 data are given in (b).

are given by Willson et al., 1982 and Fröhlich et al., 1994). However, results of the photometry of sunspots have demonstrated that the contrast of sunspots is not a constant value: it changes as a function of their area (Steiniegger et al., 1990) and the solar cycle (Maltby et al., 1986). Based on the results of photographic photometry published by Steiniegger et al. (1990), the U^2 function, used in this study, has been recalculated by Fröhlich et al. (1994). Since the solar magnetic activity is assumed to be the driving force for irradiance variability (e.g. Harvey, 1994), the full disk magnetic flux measured at the National Solar Observatory at Kitt Peak is included in our analysis and it has been directly compared to the irradiance data.

3 Time series and their uncertainties

3.1 Study the daily standard deviations of total solar irradiance

The SMM/ACRIM 1 daily mean values and their standard deviations (thereafter STD) are plotted in Fig. 1a for the time interval of 1980 to 1989. The STD of the SMM/ACRIM 1 data versus their daily means are presented in Fig. 1b. As can be seen from Fig. 1a, total solar irradiance continuously decreased from the maximum of solar cycle 21 (1980) towards solar minimum and started to rise in early 1987 with the ascending phase of solar cycle 22 (Willson and Willson, 1988). The increased measuring uncertainty during the spin operational mode of the SMM satellite is clearly seen in Fig. 1a. In order to study the variability of STD in

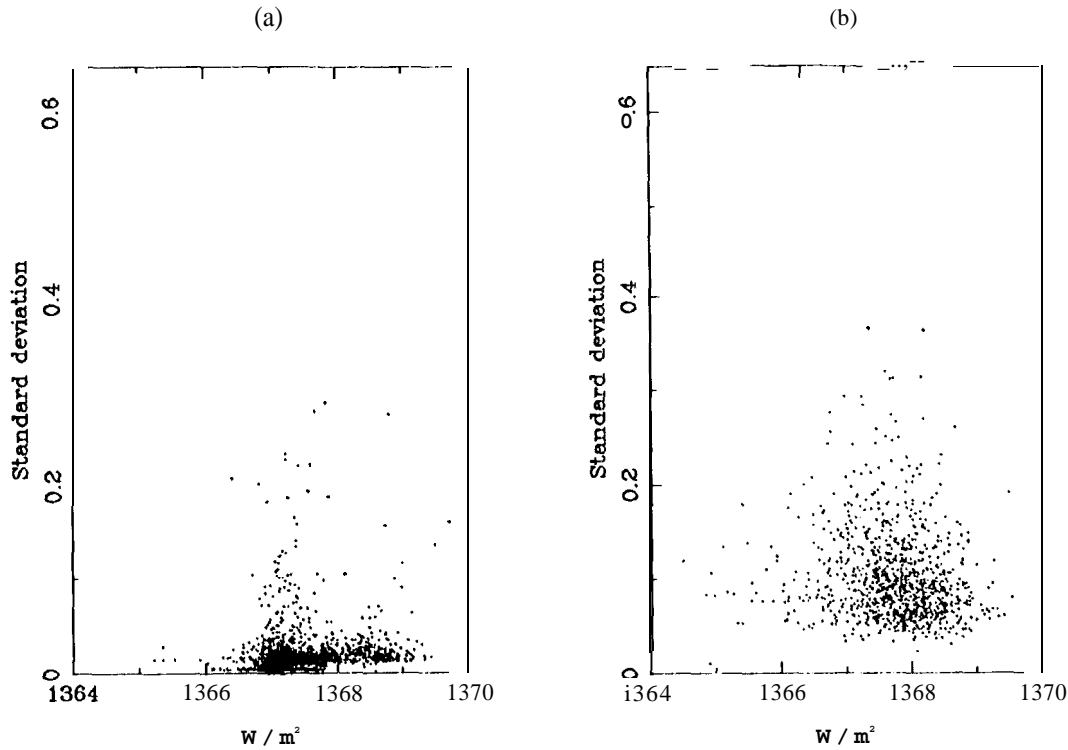


Figure 2: The standard deviations of the ACRIM 1 data versus the daily irradiance values during the normal operational mode of the satellite are plotted in (a); the same is shown for the spin operational mode (b).

more detail, the normal operational and spin -mode data have been separated and their STD has been plotted against the daily mean values in Fig. 2a,b, respectively. While no particular structure can be seen in the case of the spin-mode data (Fig. 2b), the ACRIM 1 data during the normal operational mode (Fig. 2a) form a certain pattern on the scatter plot diagram of their standard deviation. Most of the irradiance values are concentrated below $0.05 W/m^2$ STD, whereas the outliers from that main cluster ($STD > 0.05$) tend to be distributed around two vertical lines. Another interesting feature of Fig. 2a is that the standard deviation less than $0.05 W/m^2$ increases with the increasing daily mean values of total irradiance. The higher irradiance values represent maximum solar activity conditions, when considerable changes are observed in total irradiance within a day due to the formation and evolution of big complex active regions. Because of the larger daily irradiance variability, the standard deviation of the data is higher than during minimum activity conditions, when only a few and small active regions occur on the Sun.

To further investigate the physical nature of the pattern observed in the normal mode of ACRIM 1 data, the quiet- and active-Sun irradiance values and their standard deviations have been separated. The quiet- Sun irradiance values have been chosen for the time interval of July 1, 1984 to September 30, 1986, when total solar irradiance showed only a small variability around its mean value. There was an obvious decline in solar activity in July 1984 and after this time only small sunspots occurred on the Sun. Although the magnetic solar minimum occurred in September 1986, in October large active regions, already belonging to solar cycle 22, were

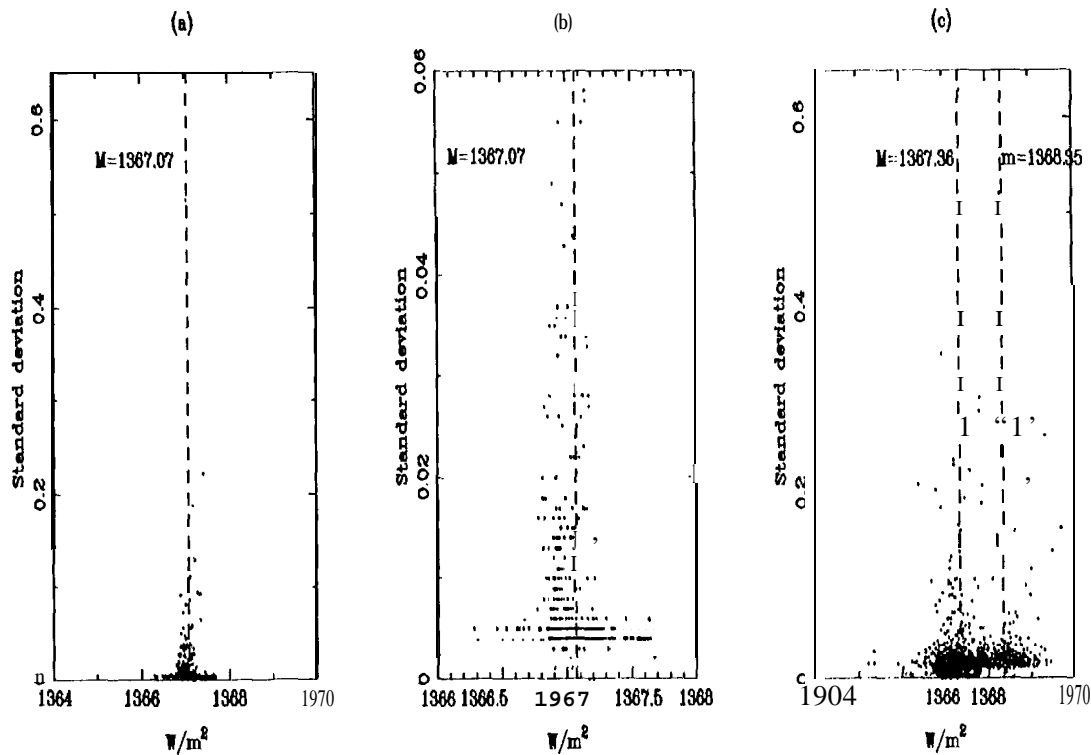


Figure 3: The standard deviations of the normal operational mode of ACRIM I data versus the daily irradiance values during solar minimum are given in (a). In (b), the plot indicates the data with STD less than $0.06 W/m^2$. (c) shows the STD against the daily active-Sun irradiance values. The vertical lines represent the mean irradiance values.

formed on the Sun and caused significant variability in both UV and total solar irradiances (Pap et al., 1990b). Irradiance values between February and December 1980 and after October 1, 1986 have been identified as active Sun values in this phase of our study.

The scatter plot diagram of the quiet-Sun irradiance values and their standard deviations are presented in Fig. 3a. The vertical line represents the mean value of the quiet-Sun irradiance ($1367.07 W/m^2$). Fig. 3b consists of a particular part of the quiet-Sun data with STD smaller than $0.06 W/m^2$. Most of these data points (74.3%) are concentrated between STD 0.004 and $0.005 W/m^2$ and these numbers essentially represent the intrinsic precision of the ACRIM I data (corresponding to 0.0004 %), in a good agreement with the published value for the average uncertainty of the ACRIM I data (better than $\pm 0.002\%$; Willson, 1984). The structures seen in Figs. 3a, b represent a Gaussian distribution of the data around their mean value. Since during solar minimum only small variability is observed in total irradiance, data points above $0.01 W/m^2$ STD represent the random noise in the data. The active-Sun values and the corresponding standard deviations are plotted in Fig. 3c and these data show a very similar pattern to that seen in Fig. 2a (data points plotted for the whole normal operational time interval). Namely, data points with STD larger than 0.05 are again distributed around two vertical lines. The first vertical line is drawn at the mean irradiance value ($M=1367.36 W/m^2$) for the rising portion of solar cycle 22 between October 1, 1986 and June 2, 1989, the end of the ACRIM I data set. The second vertical line represents the mean irradiance

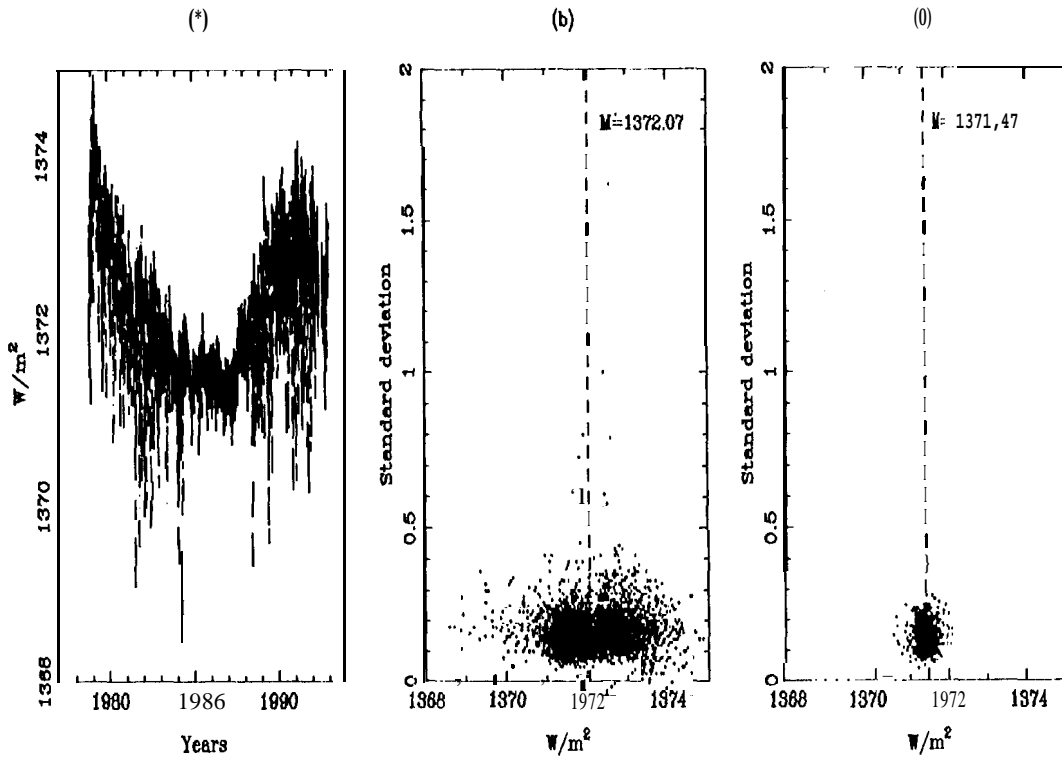


Figure 4: The daily mean values of the Nimbus-7/ERB total irradiance with their standard deviations (a). The corresponding scatter plot diagram between the $\bar{S}'(1)$ and irradiance values is plotted in (b). The scatter plot in (c) represents the minimum of solar cycle 21.

value for the maximum of solar cycle 21 in 1980 ($\bar{M} = 1368.35 W/m^2$). These two distributions represent most closely Gaussian distributions and these data ($STD > 0.05$) can again be regarded as random fluctuations in the data.

The daily Nimbus-7/ERB irradiance values with their standard deviations are presented in Fig. 4a. The ERB STD values versus the daily means are shown in Fig. 4b. As can be seen from Fig. 4, the uncertainty of the Nimbus data is much higher than that of the ACRIM 1 data due to the lack of a solar pointing platform and the limited number of observations (Hickey et al., 1988). While in the case of the normal operation of the ACRIM experiment more than 800 observations were taken within a day (Willson, 1984), the ERB experiment had a 3-day-on and 1-day-off operational mode through most of its operation and the number of observations was limited to less than a dozen per day (Hickey et al., 1988). The Nimbus-/ERB irradiance values do not show the pattern seen in the case of the normal mode of ACRIM data, instead they form a large cloud and the data are evenly distributed between $STD = 0.05$ and 0.5 similar to the spin-mode ACRIM 1 data. Fig. 4c represents the distribution of the quiet-Sun ERB values (for the same time interval as chosen for the ACRIM 1 data). Although higher irradiance values represent maximum activity conditions similar to the ACRIM 1 observations, the Gaussian distribution, that was clearly seen in the case of the normal mode of ACRIM 1 data, is not recognized in the ERB data because of their larger uncertainty. The mean $\bar{S}'(1)$ values for both the ERB and ACRIM 1 total irradiance during the quiet- and active-Sun conditions are listed in Table 1. Table 1 also contains the maximum, minimum and mean quiet- and active-Sun

<i>data</i>	min irradi	max irradi	mean irradi	111 Call STD	nb points
ACRIM1					
all	1364.479	1369.70()	1367.501	0.047	3052
spin-mode	1364.479	1369..526	1367."/30	0.104	1018
normal-mode	1365.219	1369.709	1367.387	0.018	2034
active Sun	1365.219	1369.709	1367.577	0.024	12(2
quid Sill)	1366.290	1367.672	1367.075	0.000	771
Nimbus					
all	1368.57	1374.88	1372.07	0.16	4515
activeSun	1368.57	1374.88	1372.20	0.16	3723
quiet Sun	1370.(;7	1372.11	1371.47	0.15	792

Table 1: The minimum, maximum and mean irradiance values for the SMM/ACRIM 1 and Nimbus-7/ERB irradiance values are listed together with the mean standard deviation and number of data points for the whole observing time intervals as well as for the quiet- and active-Sun periods.

irradiance values as well as the number of the corresponding data points.

3.2 Study of the monthly dispersion of the data

Since we are especially interested in the long-term irradiance variability and its relation to solar magnetic activity, any changes shorter than the solar rotational period have been considered as “noise” and removed from the data by calculating monthly averages in a similar way as published by Delache and Vigouroux (1993, 1994). This uncertainty of the monthly averages, called dispersion (111 S1), is calculated from the corresponding daily values:

$$DISP = \sqrt{\frac{\sum_{i=1}^n (D_i - \bar{D})^2}{n - 1}}$$

where D_i represents the daily data within 30 days and \bar{D} their 30 days mean.

According to the definition of the dispersion, its value represents the monthly variability of the data. In the calculation of the wavelet transforms of the investigated time series, these dispersion values will be treated as noise in a similar way as introduced by Vigouroux and Delache (1993, 1994). The dispersion values versus the monthly total irradiance averages are plotted in Fig. 5, where the quiet-Sun values are represented by crosses and the active-Sun values by dots. Note that only the ACRIM 1 data have been used in the discussions to follow since they provide a more accurate measure of the total solar energy flux than the Nimbus-

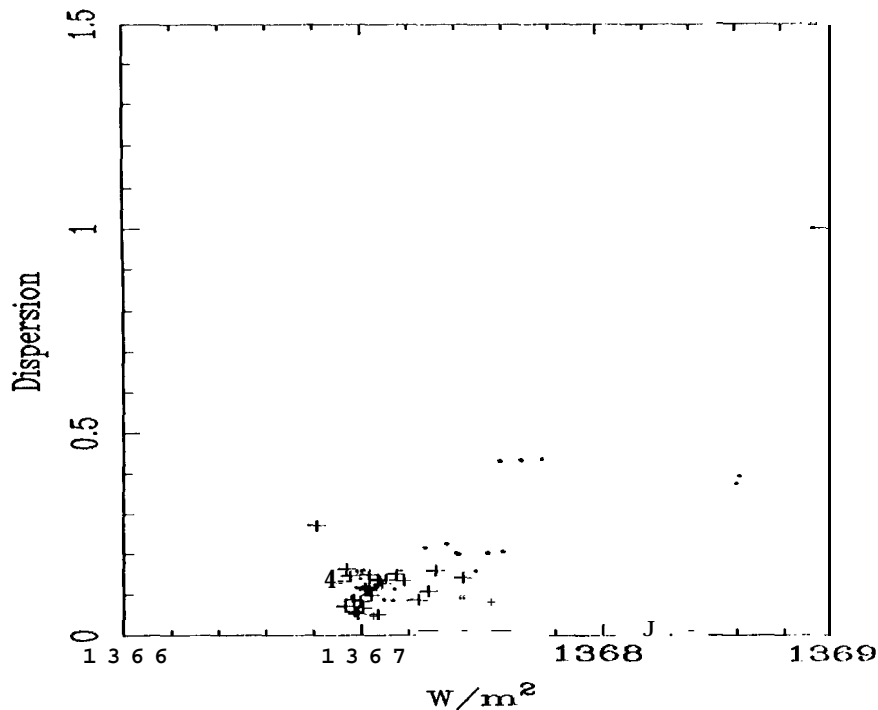


Figure 5: The dispersion values against the monthly means of the ACRIM 1 total irradiance. The crosses represent the minimum of solar cycle 21, whereas the dots refer to solar maximum activity in 1980 and the increasing solar activity conditions from October 1986 to June 1989.

7/ERB irradiance values. The dispersion values were also calculated for the spin-mode data since the monthly averages smooth out the large daily fluctuations partly arising from measuring uncertainties. As can be seen, the dispersion values are higher during active-Sun conditions, similar to the scatter plot diagrams of the STD and ACRIM 1 daily irradiance values presented in Fig. 2a and Fig. 3c. Since in this case the “error”, the calculated dispersion, means real solar variability, this confirms that the higher standard deviation of the ACRIM 1 data during higher solar activity is related more to solar effects than to instrumental uncertainties. Although the crosses, representing solar minimum activity values, are concentrated around the 1367 W/m^2 minimum irradiance value, the difference between their maximum and minimum values exceeds 0.5 W/m^2 (note that the full range of the observed solar cycle variability in the monthly averages of ACRIM total irradiance is about 1.8 W/m^2). This indicates that the solar minimum for total irradiance may not be correctly determined from a simple study of the surface manifestations of solar magnetic activity. To further examine the change of the dispersion over the solar cycle and to establish the real time of solar minimum for total solar irradiance, the dispersion diagrams have been plotted on a yearly basis (Fig. 6). As can be seen from Fig. 6, there is an obvious pattern in the ACRIM 1 dispersion diagrams and this pattern changes as a function of the solar Cycle. During solar minimum the dispersion values form a concentrated cluster of data, this feature is the most pronounced during 1986. It is interesting to note that towards maximum activity conditions this cluster is less and less compressed and the variability within the cluster shows a larger range between 0.5 and 1.4 W/m^2 . Based on the definition of the

dispersion, the variation within a particular cluster is related to the short-term changes due to the effect of active regions, whereas the change of the position of dispersion clusters over years represents the solar cycle variation in total irradiance. Therefore, study of the shape and rate of compression of the dispersion clusters may provide an additional and useful tool to estimate and predict the time of maximum and minimum solar activity conditions for solar total and UV irradiances as well as for additional solar parameters.

The dispersion values have also been calculated for the Mg c/w, PSI and magnetic flux values in order to provide an error bar for these data since no standard deviations are available for their daily values (either because they are not published or because there are only 1-2 observations per day). Besides providing error bars for the wavelet analysis, the dispersion diagrams have also been examined to clarify whether the cluster structure found in the case of the ACRI M data is a general pattern for other solar indices. To directly compare the temporal variation of total solar and UV irradiances, the effect of sunspots has been removed from total irradiance by means of the PSI function. The time series of total irradiance corrected for sunspot darkening ($S_c = \text{ACRI M} + \text{PSI}$), the Mg c/w ratio, PSI and the full disk magnetic flux are presented in Fig. 7(a) to (d). It is interesting to note that while the maximum activity level for UV irradiance is almost identical during solar cycles 21 and 22, the strength of the magnetic flux is much higher during the maximum of cycle 22 than during cycle 21. An additional difference is obvious from these time series: the UV irradiance reaches maximum activity values before the magnetic flux during both solar cycles. In addition, both UV and total irradiance corrected for sunspot darkening start to rise prior to the magnetic flux at the beginning of the ascending phase of solar cycle 22, as has already been pointed out by Papet et al. (1995).

The yearly dispersion diagrams of the Mg c/w ratio from 1979 to 1994 are presented in Figs. 8 and 9. As can be seen, the dispersion of the Mg c/w data also forms a cluster structure, similar to total irradiance. It is interesting to note that between 1979 and 1981 the shape of these clusters is almost vertical and the data points fluctuate around 0.28. This structure demonstrates that the Mg c/w had about a 3-year-long flat maximum variability during solar cycle 21. The dispersion cluster started to move toward lower Mg c/w values in 1982, although the extended shape of the cluster indicates that the short-term variability still was significant at the beginning of the declining phase of solar cycle 21. The dispersion clusters had become compressed by 1984, however these clusters were never as compressed as the ones for total irradiance during minimum activity conditions. This feature indicates that the short-term UV variability is significantly higher during minimum activity condition than is the total solar flux. These dispersion diagrams place the minimum time of UV irradiance in 1985 and 1986, and as can be seen from Fig. 8, a slight increase in the Mg c/w started in 1987. The pattern in the dispersion diagrams for 1989 to 1991 (see Fig. 9) was very similar to that of the maximum of cycle 21, demonstrating that the two maxima of solar cycles 21 and 22 were almost identical in the case of the UV flux. The dispersion diagram for 1992 shows that a sudden decrease in the UV irradiance occurred during this period and the amplitude of this decrease was as large

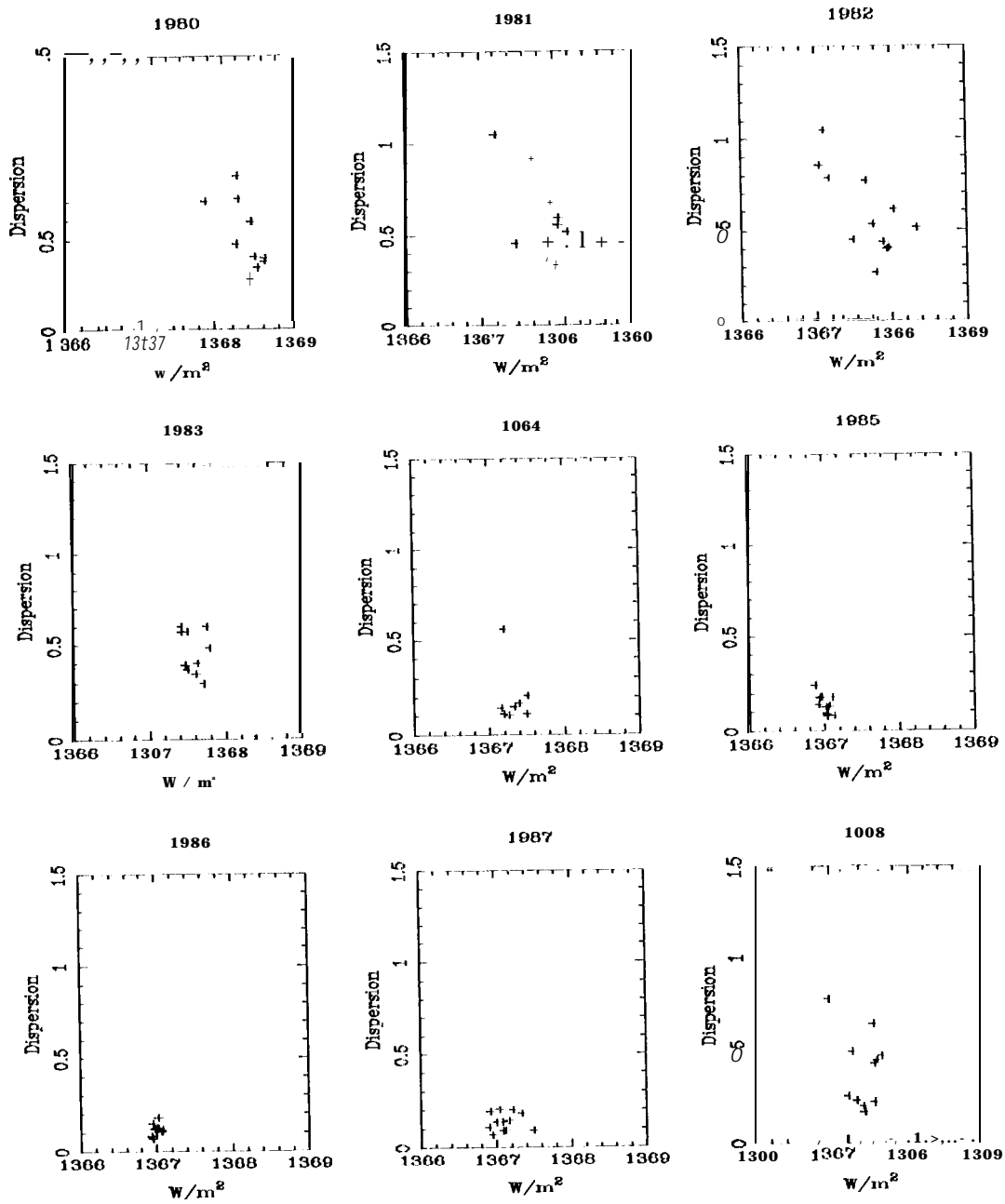


Figure 6: The yearly ACRIM 1 total solar irradiance dispersion diagrams between 1980 and 1989.

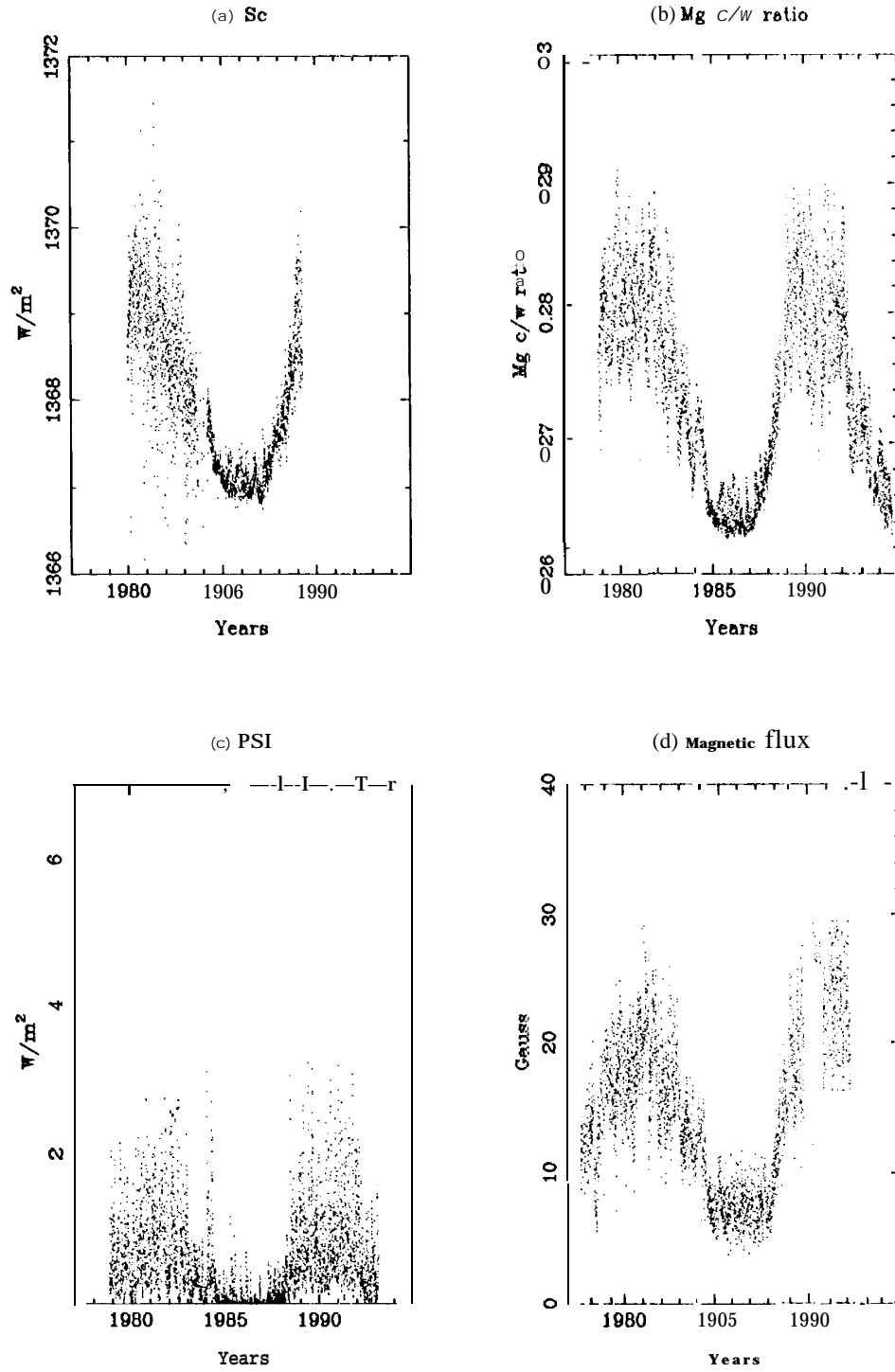


Figure 7: Time series of the ACRIM I + PSI (a), combined Nimbus-7/NOAA9 Mg c/w ratio (b), PSI (c), and the full disk magnetic flux (d).

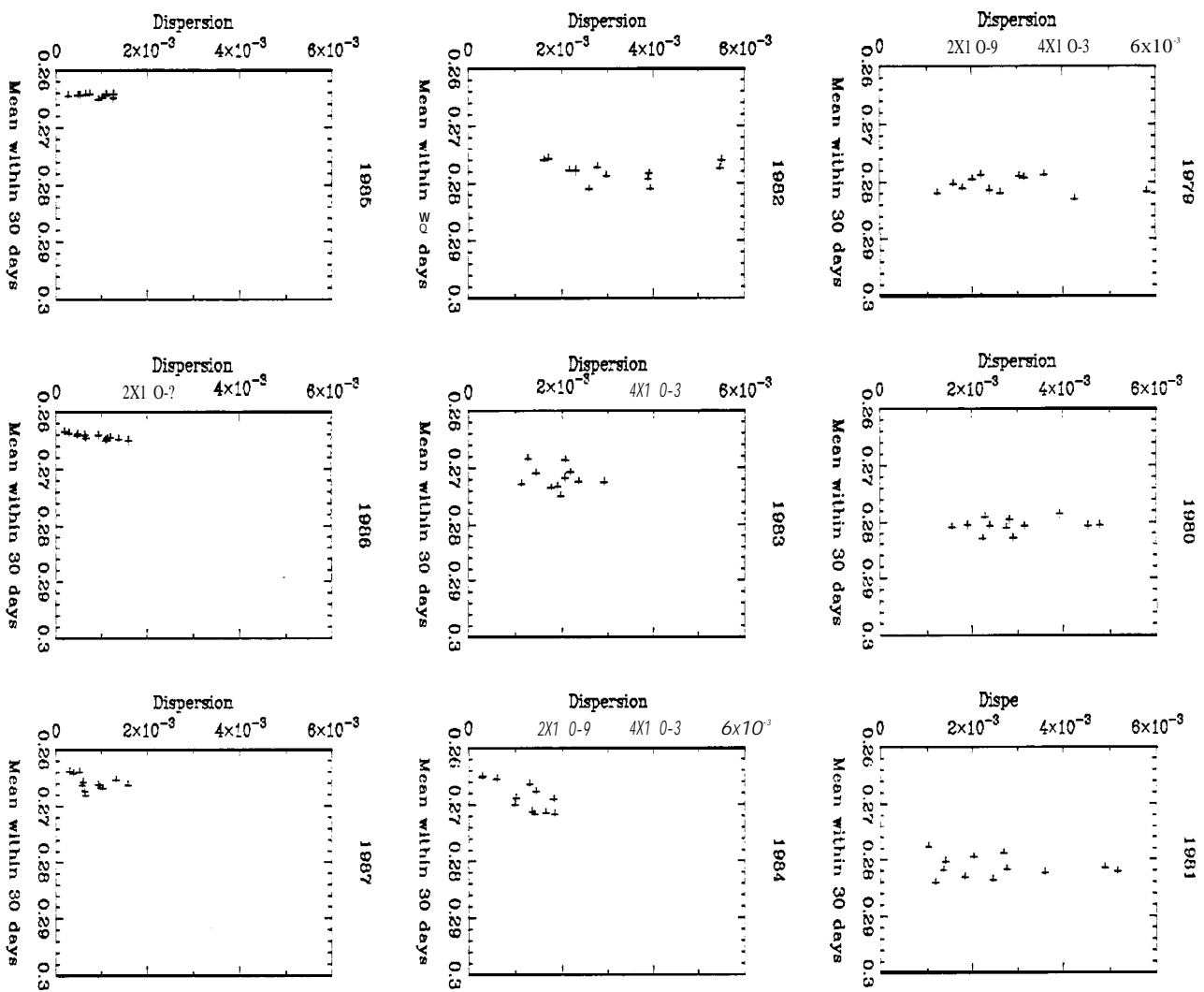


Figure 8: The yearly Mg c/w ratio dispersion diagrams (from 1979 to 1987)

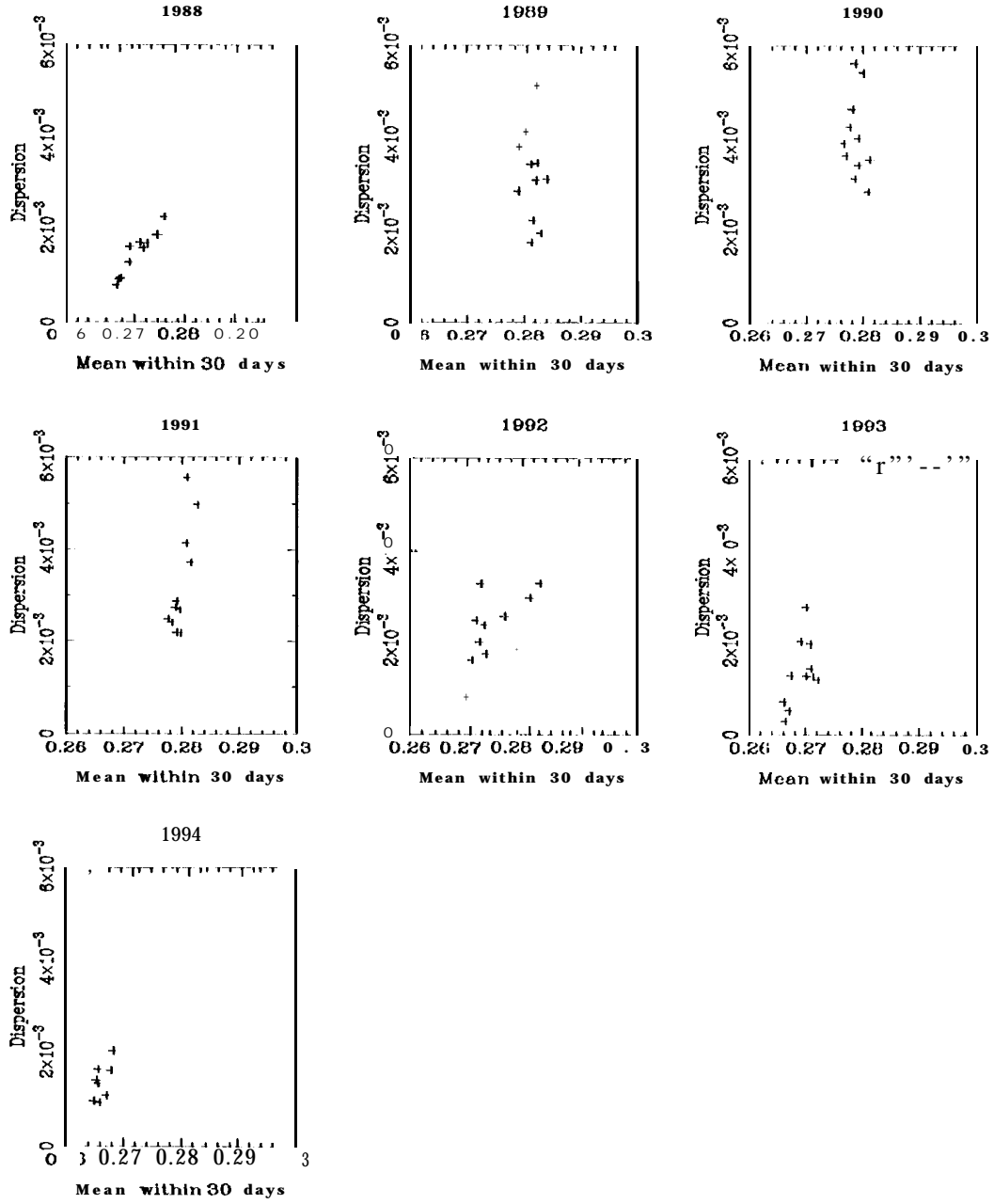


Figure 9: The yearly Mg c/w ratio dispersion diagrams (from 1988 to 1994).

as that of the observed decline between early 1982 and the end of 1983. This sudden decrease of UV irradiance happened between February and June of 1992 (White et al., 1994) and was caused by the disappearance of the magnetic activity in the southern solar hemisphere (Harvey, 1994). It is interesting to note that the structure of the dispersion diagram of the Mg c/w ratio during 1994 is very similar to the dispersion diagram for 1985-1986 indicating that the UV irradiance may have already reached the minimum activity conditions of solar cycle 22 or its value is very close to the minimum value observed during solar cycle 21. However, it must be kept in mind that this prediction is based on studying a data set covering only one and a half solar cycles. Considering that the variability in solar UV (and total) irradiance may be different from one cycle to another one, further studies of solar irradiance time series covering several solar cycles are required to develop a statistically significant method for predicting accurately the maximum and minimum activity conditions.

We note that similar clusters have been found in the rest of the investigated data, indicating that the dispersion diagrams provide a helpful tool in studying long-term changes in various solar activity indices. In the discussion to follow we will concentrate only on the structure of the dispersion diagrams during minimum activity conditions in order to better estimate the minimum time of solar total and UV irradiances and the measures of the solar magnetic activity. Fig. 10 shows the dispersion diagrams for the ACRIM 1 total irradiance (a), Sc (b), Mg c/w (c), $1'S1$ (d), and the magnetic flux (e). The dots represent data for 1984, crosses for 1985, diamonds for 1986, and stars for 1987. As the distribution of the dots (data for 1984) shows in Fig. 10, part of 1984 belonged to the declining portion of solar cycle 21. The beginning of the minimum of solar cycle 21 has been determined for each data set by studying the distribution of the dots on a monthly basis. The ending date of solar minimum has been determined in a similar fashion: the distribution of stars (representing data points for 1987) made it possible to determine whether these data belonged to the cluster of minimum activity values. The estimated solar minimum intervals (beginning and ending dates) and the length of the minimum of solar cycle 21 for solar total and UV irradiances as well as for the magnetic surrogates are listed in Table 2. These results give an additional evidence that solar indices representing strong magnetic field, such as the full disk magnetic flux and $1'S1$, reach minimum activity conditions a few months before solar irradiances and both total and UV irradiances start to rise prior to the magnetic flux at the beginning of solar cycle 22 (Pap et al., 1995).

Figs. 11(a)-(e) show the dispersion diagrams of the ACRIM 1 (a), Sc (b), Mg c/w (c), $1'S1$ (d), and the magnetic flux (e), including both quiet- and active-Sun values. The crosses on each plot represent the minimum activity conditions for the time intervals shown in Table 1 and the dots indicate the active-Sun values including data for maximum solar activity conditions as well as for the decline and rise of solar cycles 21 and 22. **Note** that the investigated time series cover different time intervals and this does not allow a detailed analysis of the dispersion diagrams for maximum solar activity. This is especially true for total solar irradiance, for which there are no high precision observations covering the whole time interval of the maxima of solar

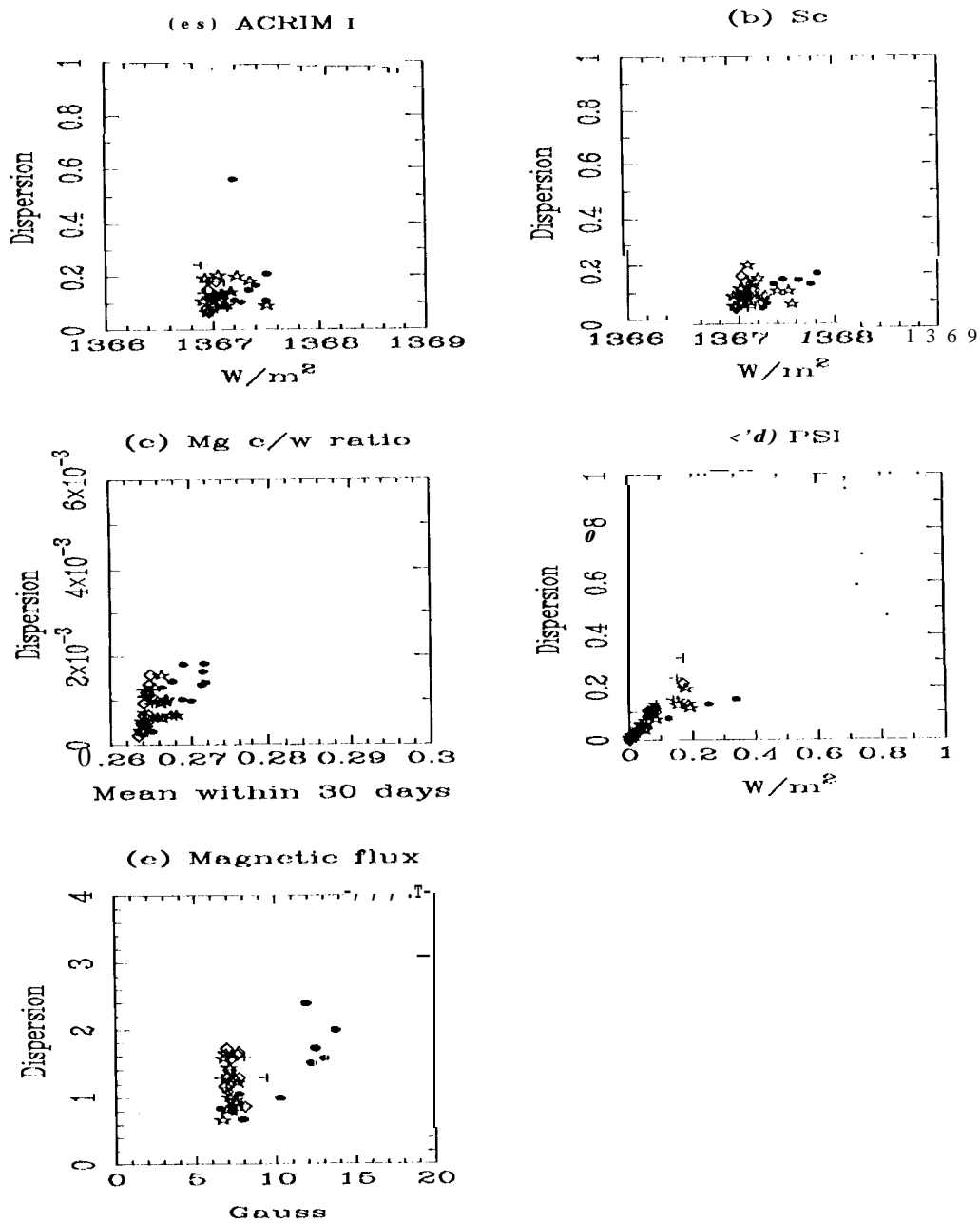


Figure 10: Dispersion diagrams for ACRIM 1 (a), Sc (b), Mg c/w ratio (c), PSI (d) and the full disk magnetic flux (e) for minimum solar activity conditions. The dots represents data for 1984, crosses for 1985, diamonds for 1986 and stars for 1987.

Time Series	Beginning of Minimum	End of Minimum	Length
ACRIM1	January 1985	August, 1987	32 months
ACRIM1 + 1'S1	January 1985	March 1987	27 months
1's1	August 1984	October 1987	391110111,11s
Mg c/w	January 1985	March 1987	27 months
Magn. field	August 1984	December 1987	41 months

Table 2: The beginning and ending dates of minimum solar activity conditions during solar cycle 21 for the investigated time series. These dates were estimated from analyzing the time series as well as from the dispersion diagrams presented in Fig. 10. The length of the estimated solar minimum is also given in months.

Cycles 21 and 22.

As can be seen from Figs. 11(a)-(c), the relation between the dispersion, “the error bar”, and the monthly averages of the data is quite different for solar minimum and active-sun conditions. In the case of solar irradiance (both bolometric and the UV flux) as well as the magnetic flux data, the minimum values are concentrated along almost a vertical line indicating the fluctuations of these data around their mean at the time of solar minimum. In contrast, in the case of the PSI function the regression lines for both quiet- and active-Sun conditions converge towards zero because the value of PSI is always zero in the absence of sunspots, independent of the phase of the solar activity cycle. Another interesting feature can be recognized in these dispersion diagrams, namely the scatter of the data is much larger for higher data values. This arises from the larger variability in the data during solar maximum due to the changes on active region time scales. This feature is most obvious in the case of the Mg c/w. The distribution of the maximum values of the Mg c/w ratio is related to the several years long maximum activity of both solar cycles 21 and 22, as has already been seen in Fig. 6. These results indicate that the error bars calculated from the monthly averages of the data depend on the phase of the solar cycle and this fact has to be taken into account when the significant components of the Fourier and/or wavelet transforms above the noise level are calculated from the time series. Application of the results discussed in this paper to the wavelet analysis will be presented in the second part of our paper and this analysis will lead to a better understanding of the discrepancies found between observed and modelled irradiance values.

4 Conclusions

Although considerable information exists on solar irradiance variability, the underlying physical processes are not well understood. It has not yet been clarified whether the residual variations

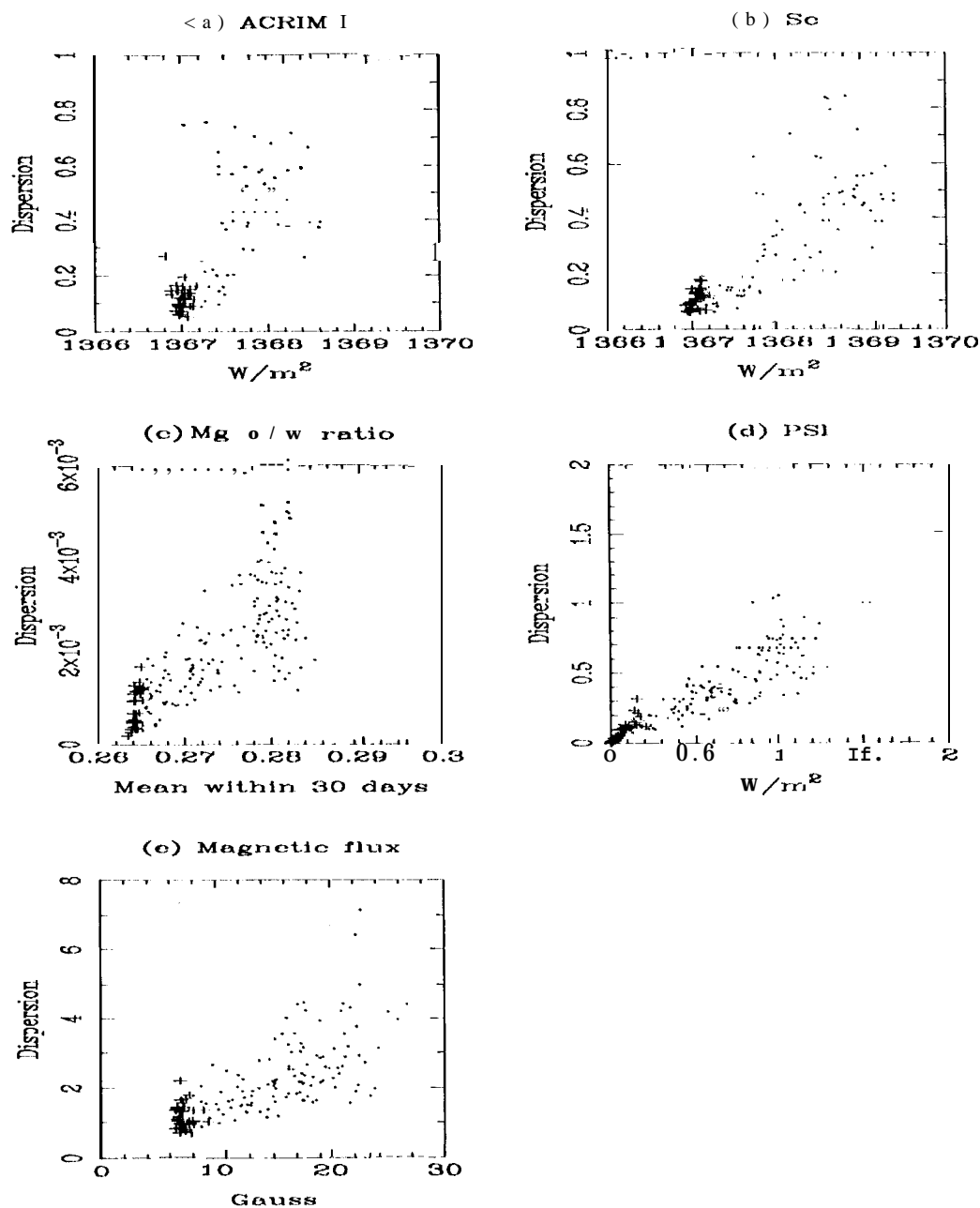


Figure 1 E: Dispersion diagrams for ACRIM 1 (a), Sc (b), Mg c/w ratio (c), 1'S1 (d) and the full disk magnetic flux (e) For each figure the cloud of (ross corresponds to the minimum of the cycle 21, as defined in Table II, the cloud of points corresponds to the active phase of the Sun.

in total and UV irradiances after removing the effect of sunspots and bright magnetic features (see Pap and Fröhlich, 1992) are related to real solar effects or they are simply determined by a noise component in the data. In this paper we have applied a new method, following the original idea of Vigouroux and Delache (1994), to evaluate and understand the uncertainties in solar irradiance (both bolometric and UV flux) and magnetic activity indices, such as the PSI function and the full disk magnetic flux. It has been shown that investigations of the scatter plot diagrams between daily solar irradiance measurements and their standard deviations provide an important tool to separate the random fluctuations related to instrumental effects from real solar variations.

In order to provide error bars for the wavelet analysis, to be described in the second part of this paper, the short-term variations were removed from the data by creating monthly averages. The distribution of this "solar noise" has been studied in detail in this paper. It has been demonstrated that the dispersion diagrams contain important information about the long-term changes in various solar activity indices. A cluster structure of these diagrams has been discovered and it is shown that the shape and the compression of these clusters change as a function of the solar cycle. These investigations can provide an important new technique in predicting the time behavior of solar activity indices and estimating the occurrence of the maximum and minimum of solar cycle. Our results confirm that the length of the solar minimum is different for solar total and UV irradiances and the measures of solar magnetic activity and that there is a phase shift between the changes in the solar magnetic flux and solar irradiance at the beginning and the end of solar minimum as was found by Pap et al. (1995).

In the second part of our paper, we will examine the variations in solar irradiance and measures of the solar magnetic activity with a wavelet technique. Using the error bars determined from the statistical properties of the data in the current analysis, we will invert the wavelet transforms that contain only the significant solar components in order to better understand the relation between solar magnetic activity and irradiance variability.

Acknowledgements: The research described in this paper was carried out by the Jet Propulsion Laboratory, California Institute of Technology under a contract with the National Aeronautics and Space Administration (J. M. Pap) and by the laboratoire Cassini, associé au C.N.R.S. (U.R.A. 1362) of the Observatoire de la Côte d'Azur (A. Vigouroux). The SMM/ACRIM I data used in this study have been produced by the Active Cavity Radiometer Irradiance Monitoring Group at JPL. The Nimbus-7/ERB data were kindly provided by Dr. D. Hoyt. The NOAA/SOLAR Mg c/w ratio have been processed at NOAA/SEL and were provided by J. Puga for this analysis. The NSO/Kitt Peak magnetic data used here are produced cooperatively by NSF/NOAO, NASA/GSFC and NOAA/SEL and provided by courtesy of Dr. J. Harvey. The useful comments of Drs. R.F. Donnelly, E. Fossat and L. Puga are highly appreciated.

References

- Barth, C. A., K. Tobiska, G. Rottman, and O.R. White, Comparison of 10.7 cm radio flux with SML solar Lyman alpha flux, *Geophys. Res. Lett.*, **17**, 571-574, 1990.
- Bouwer, D., Periodicities of solar irradiance and solar activity indices, **1**, *Solar Physics*, **142**, 365-389, **1992**.
- Brandt, P. N., M. Stix, and W. Weinhardt, Modelling solar irradiance with an area depended photometric sunspot index, *Solar Physics*, **152**, 119-124, 1994.
- Cebula, R.P., E. Hilsenrath, and M.T. Deland, Middle ultraviolet solar spectral irradiance measurements, 1985-1992, from the SBUV/2 and SSBUV instruments, In *The Sun as a Variable Star: Solar and Stellar Irradiance Variations* (eds. J. M. Pap, C. Fröhlich, H.S. Hudson, and S.K. Solanki), Cambridge Univ. Press., 81-88, 1994.
- Donnelly, R.F., *Handbook*, for MAP (eds. J. Lastovicka, T. Miles, and A. O'Neill), **29**, 1, 1989.
- Donnelly, R.F., Solar UV spectral irradiance variations, *J. Geomagnet. Geoelect.*, **43 Suppl.**, 835-843, 1991.
- Donnelly, R.F., O.R. White, and W.C. Livingston, The solar Ca II K index and the Mg II core-to-wing ratio, *Solar Physics*, **152**, 69-76, 1994.
- Foukal, P. and J. Lean, Magnetic modulation of solar luminosity by photospheric activity, *Ap.J.*, **328**, 347-357, 1988.
- Fröhlich, C. and J. Pap, Multispectral analysis of total solar irradiance variations) *Astron. Astrophys.*, **220**, 272-280, 1989.
- Fröhlich, C., J. Pap, and H. S. Hudson, Improvement of the Photometric sunspot index and the changes of the sunspot contrast within the solar cycle, *Solar Physics*, **152**, 111-118, 1994.
- Harvey, K., Irradiance models based on solar magnetic fields, In *The Sun as a Variable Star: Solar and Stellar Irradiance Variations* (eds. J.M. Pap, C. Fröhlich, H.S. Hudson, and S.K. Solanki), Cambridge Univ. Press., 217-225, 1994.
- Heath, D. H. and B. M. Schlesinger, The Mg 280-11111 doublet as a monitor of changes in solar ultraviolet irradiance, *J. Geophys. Res.*, **91**, 8672-, "1986.
- Hickey, J.R., B.M. Alton, H.L. Kyle, and D.V. Hoyt, Total solar irradiance measurements by ERB/Nimbus-7. A review of nine years, *Space Sci. Rev.*, **48**, 321-342, 1988.
- Hoyt, D. V., H.L. Kyle, J. H. Hickey, and R.H. Maschhoff, The Nimbus-7 solar total irradiance: A new algorithm for its derivation, *J. Geophys. Res.*, **97**, 51-63, 1992.
- Hudson, H. S., Observed variability of the solar luminosity, *Ann. Revs. Astron. Astrophys.*, **26**, 473-507, 1988.
- Hudson, H. S., S. Silva, M. Woodard, and R. C. Willson, The effects of sunspots on solar irradiance, *Solar Physics*, **76**, 211-218, 1982.
- Kuhn, J., K.G. Libbrecht, and R. Dicke, The surface temperature of the Sun and changes in the solar constant, *Science*, **242**, **908-911**, 1988.
- Kyle, H.L., D.V. Hoyt, J.R. Hickey, R.H. Maschhoff, and B.J. Vallete, Nimbus-7 Earth Radia-

- tion Budget Calibration History - Part 1: The solar channels, *NASA Reference Publ. 1316*, GSC, Greenbelt, 1993.
- Lean, J., Solar UV variations, *J. Geophys. Res.*, **92**, 839-868, 1987.
- Lean, J., Variations in the Sun's radiative output, *Rev. Geophys.*, **29**, 505-535, 1991.
- Lean, J. and T.P. Repoff, A statistical analysis of solar flux variations over time scales of solar rotation: 1978-1982, *J. Geophys. Res.*, **92**, 5555-5568, 1987.
- Maltby, P., E.H. Avrett, M. Carlsson, Kjeldseth-Moc, R.L. Kurucz, and R. Looser, New sunspot umbral model and its variation with the solar cycle, *Ap. J.*, **306**, 284-303, 1986.
- Pap, J., Variations in solar Lyman alpha irradiance on short time scale, *Astron. Astrophys.*, **264**, 249-259, 1992.
- Pap, J. and C. Fröhlich, Multivariate spectral analysis of short-term irradiance variations, In *Proc. Solar Electromagnetic Radiation Study for Solar Cycle 22*, (eds. H. D. Donnelly), SEL, NOAA/ERL, Boulder, 62-75, 1992.
- Pap, J. and O.R. White, Panel discussion on total solar irradiance variations and the Maunder Minimum, In *Proc. of NA TO Advanced Research Workshop on the Solar Engine and its Influence on Terrestrial Atmosphere and Climate*, (eds. E. Ribes), Kluwer Academic Press, in press, 1994.
- Pap, J., L. Tobiska, and D. Bouwer, Periodicities of solar irradiance and solar activity indices, *I. Solar Physics*, **129**, 165-189, 1990a.
- Pap, J., W.J.J. Marquette, and R.F. Donnelly, Modelling solar irradiances using ground-based measurements, *Adv. Space Res.*, **11**, 271-275, 1990b.
- Pap, J., J. London, and G.A. Rottman, Variability of UV irradiance at Lyman alpha and total solar irradiance, *Astron. Astrophys.*, **245**, 648-653, 1991.
- Pap, J., R.C. Willson, C. Fröhlich, R.F. Donnelly, and L. Puga, Long-term variations in total solar irradiance, *Solar Physics*, **152**, 13-21, 1994.
- Pap, J., A. Ruzmaikin, R. Kariyappa, L. Puga, and R.C. Willson, Is there a phase shift between the full disk solar magnetic flux and solar irradiance?, *Solar Physics*, submitted, 1995.
- Priestly, M.B., A short history of time series, Paper presented at the *International Conference on Applications of Time Series Analysis in Astronomy and Meteorology*, Padua, Sept. 1993.
- Ribes, E., P. Mein, and A. Mangeney, A large scale meridional circulation in the convection zone, *Nature*, **318**, 170-171, 1985.
- Scargle, J.D., Wavelet methods in astronomical time series analysis, Paper presented at the *International Conference on Applications of Time Series Analysis in Astronomy and Meteorology*, Padua, Sept. 1993.
- Schlesinger, B.M. and R.L. Cebula, Solar variations 1978-1987 estimated from an empirical model for changes with time in the sensitivity of the Solar Backscatter Ultraviolet Instrument, *J. Geophys. Res.*, **97**, 10119-10134, 1992.
- Steinberger, M., J. Brandt, J. Pap, and W. Schmidt, Sunspot photometry and the total solar irradiance deficit measured in 1980 by ACRIM, *Astrophys. Space Sci.*, **170**, 127-133, 1990.

- Vigouroux, A. and Ph. Delache, Fourier versus wavelet analysis of solar diameter variability, *Astron. Astrophys.*, **278**, 607-616, 1993.
- Vigouroux, A. and Ph. Delache, Sunspot number uncertainties and parametric representations of solar activity variations, *Solar Physics*, **152**, 267-274, 1991.
- White, O.L., G.J. Rottman, P. Woods, S. Keil, W.C. Livingston, K.F. Fapping, R.F. Donnelly, and L. Puga, Change in the UV output of the Sun in 1992 and its effect in the thermosphere, *J. Geophys. Res.*, 1994.
- Willson, R. C., Measurements of solar total irradiance and its variability, *Space Sci. Rev.*, **38**, 203-242, 1984.
- Willson, R. C. and H. S. Hudson, Solar luminosity variations in solar cycle 21, *Nature*, **351**, 42-44, 1988.
- Willson, R. C. and H. S. Hudson, The Sun's luminosity over a complete solar cycle, *Nature*, **351**, 42-44, 1991.
- Willson R. C., S. Gulkis, M. Janssen, H. S. Hudson, and G. A. Chapman, Observations of solar irradiance variability, *Science*, **211**, 700-702, 1981.